Supporting Information for

An artificial aluminum-tin alloy layer on aluminum metal anodes for ultra-stable rechargeable aluminum-ion batteries

Xiao Wang[1], Chen Zhao[1], Peng Luo[2], Yan Xin[1*], Yunnian Ge[1], Huajun Tian [1*]

[1] Key Laboratory of Power Station Energy Transfer Conversion and System of Ministry of Education and School of Energy Power and Mechanical Engineering, and Beijing Laboratory of New Energy Storage Technology, North China Electric Power University, Beijing, 102206, China

[2] Institute of Digital Technology, State Grid Digital Technology Holding Co. Ltd.

*E-mail: xinyan@ncepu.edu.cn； Huajun.Tian@ncepu.edu.cn

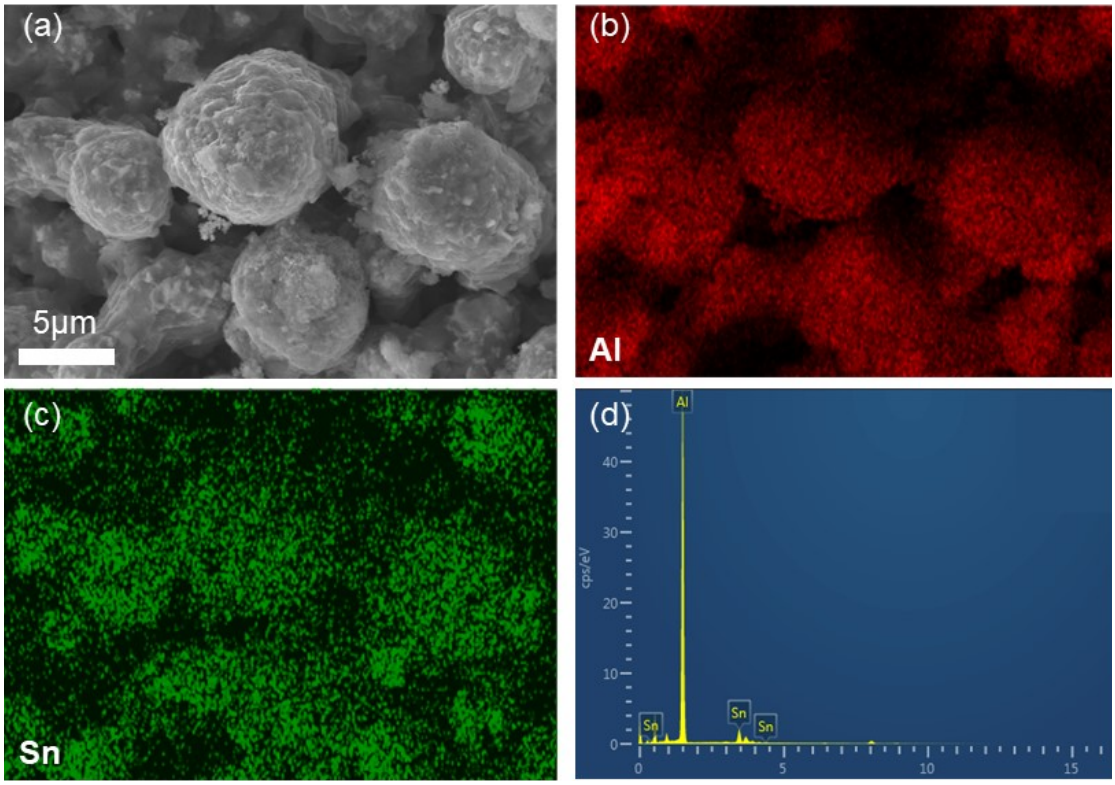

Figure S1. (a) Top-view SEM image of AlSn@Cu anode obtained by the electrodeposition, corresponding EDS mappings of (b) Al, (c) Sn, and (d) EDS spectrum.

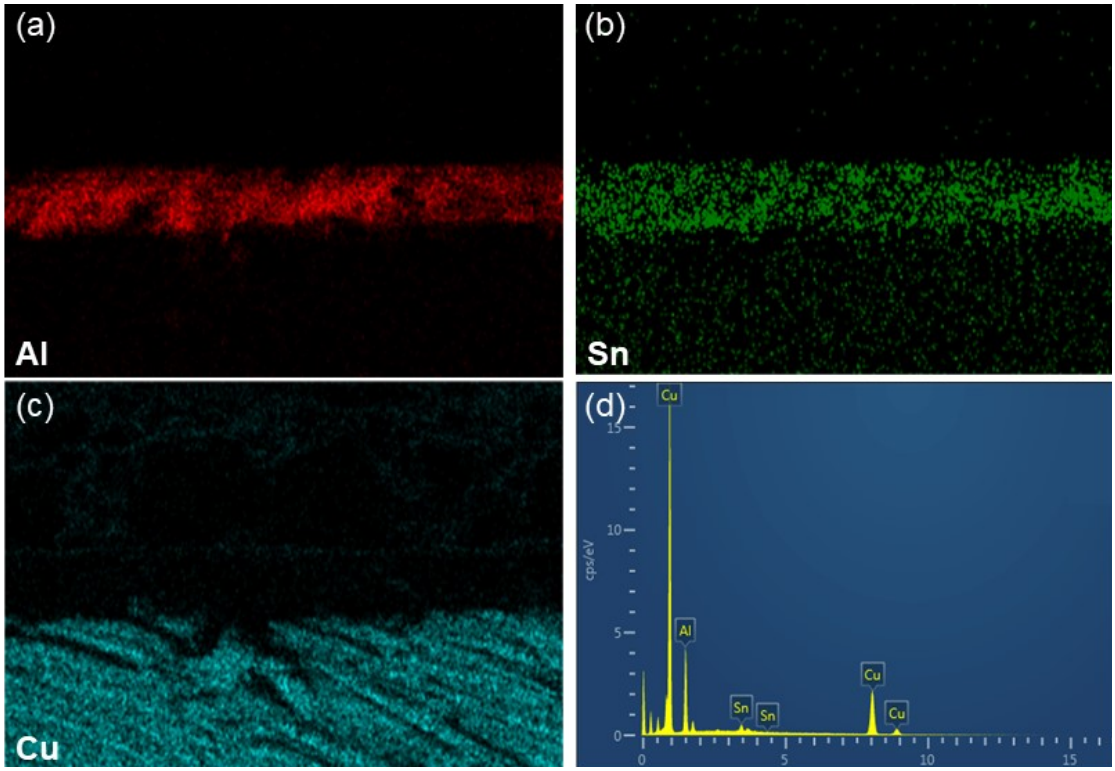

Figure S2. EDS mappings of (a)Al, (b) Sn, (c) Cu and (d) EDS spectrum corresponding to the cross-section SEM image.

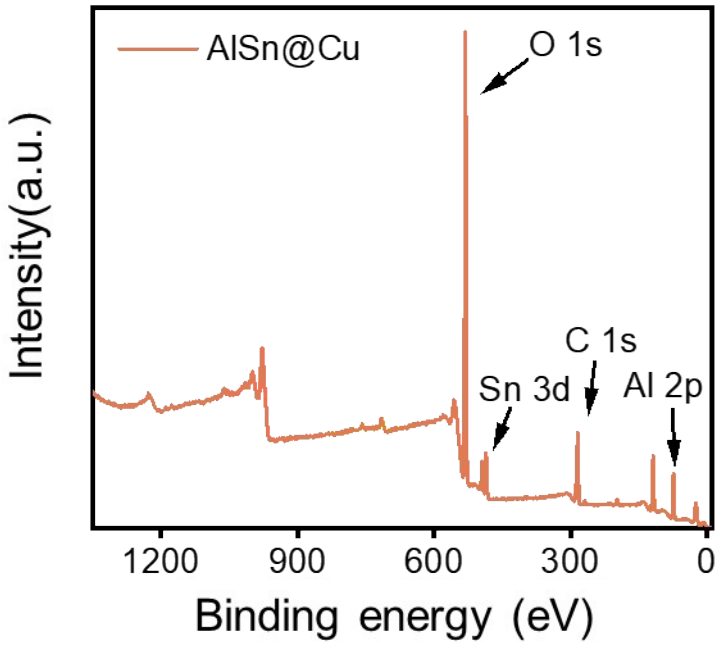

Figure S3. XPS survey spectrum of AlSn@Cu anode.

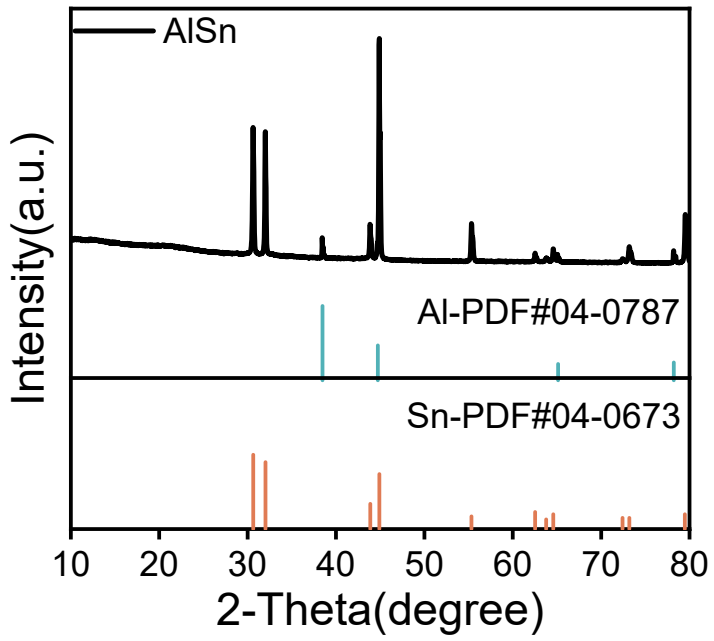

Figure S4. XRD patterns of AlSn alloys prepared by vacuum arc melting, which can be aligned to standard cards of Al (PDF#04-0787) and Sn (PDF#04-0673).

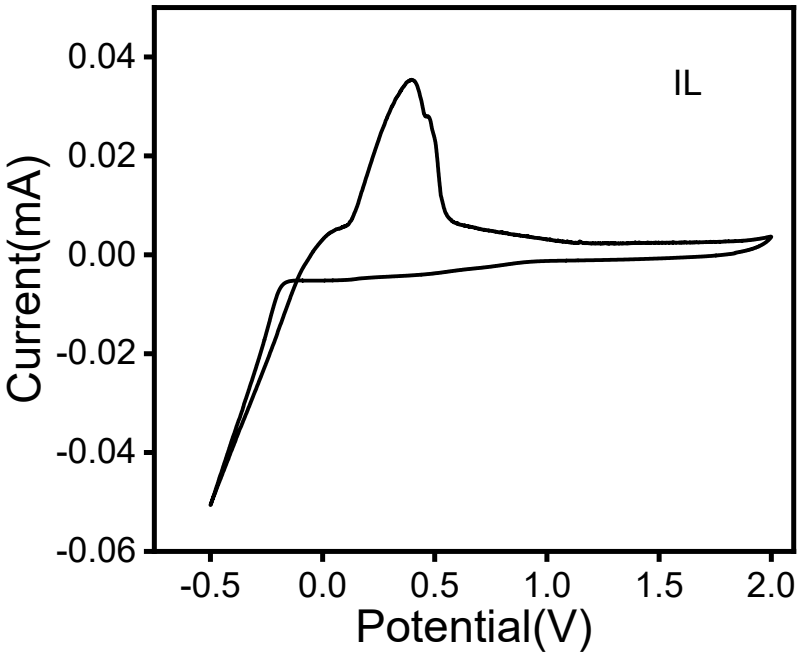

Figure S5. Electrochemical performance of the IL electrolyte in a three-electrode set-up. Working electrode: Pt, Reference electrode: AlSn@Cu anode, Counter electrode: AlSn@Cu anode.

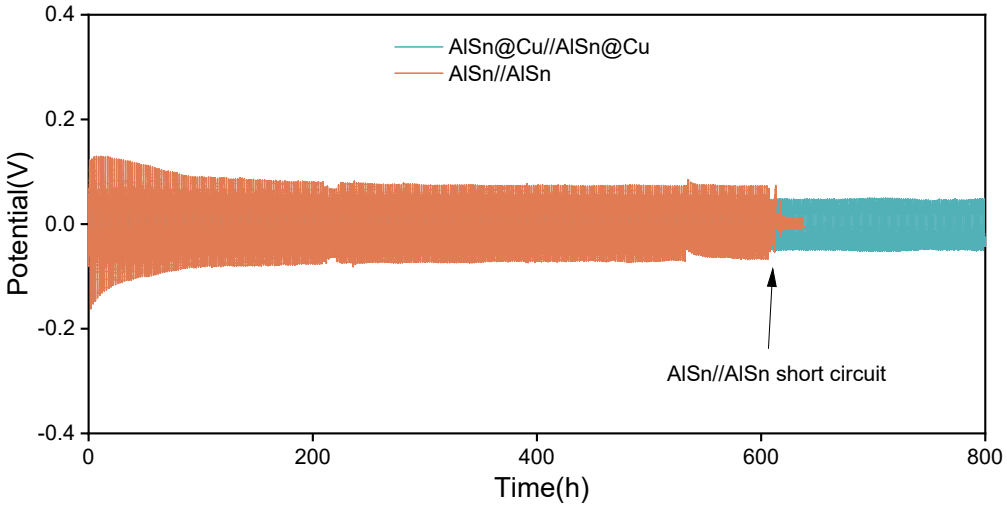

Figure S6. Long cycle curves of symmetric AlSn@Cu and AlSn cells at a current density of 0.5 mA cm^{-2}.

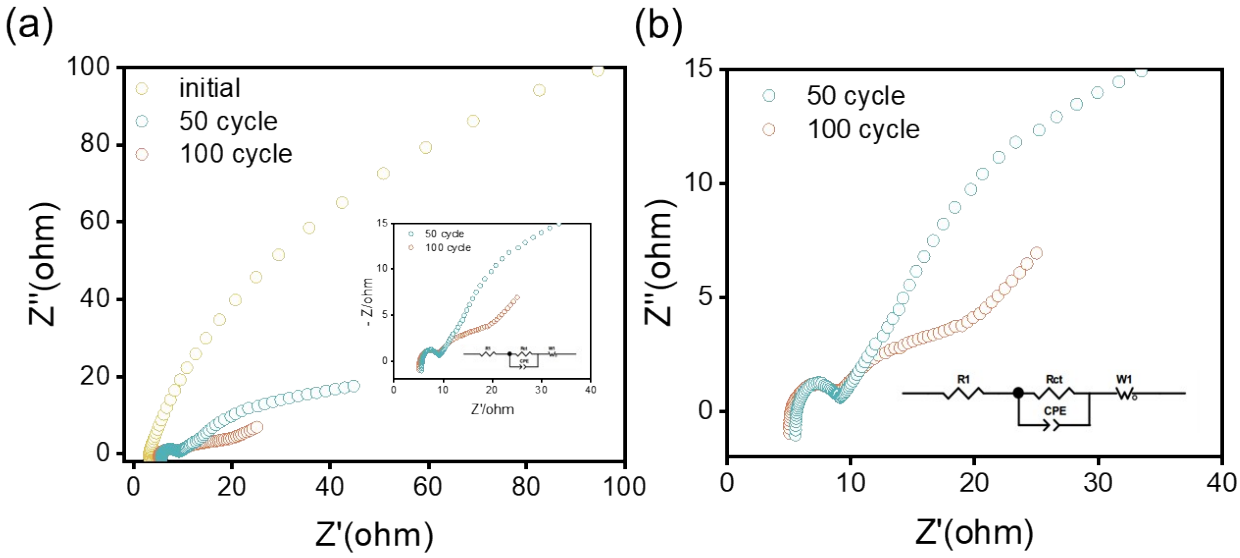

Figure S7. (a) EIS plots of symmetric AlSn@Cu cell in initial and after different cycles. (b) Enlarged images of EIS of symmetric AlSn@Cu cell after 50 and 100 cycles.

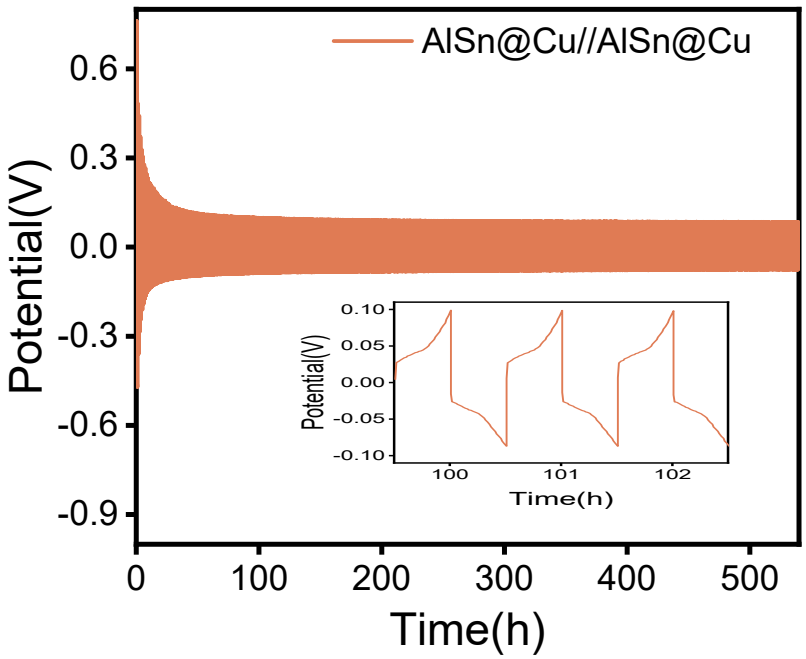

Figure S8. Long cycle curves of symmetric AlSn@Cu cell at low temperature -15°C at a current density of 0.2 mA cm^{-2}.

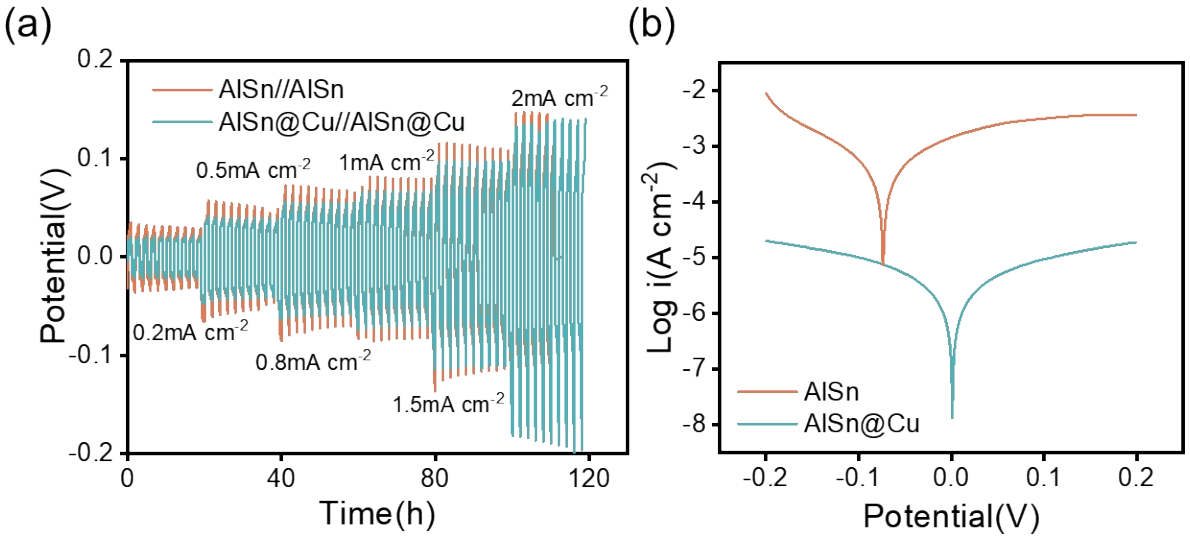

Figure S9. (a) Rate capability of symmetric AlSn@Cu and AlSn cells at current densities of 0.2~2 mA cm^{-2}. (b) Tafel curves of the AlSn and AlSn@Cu.

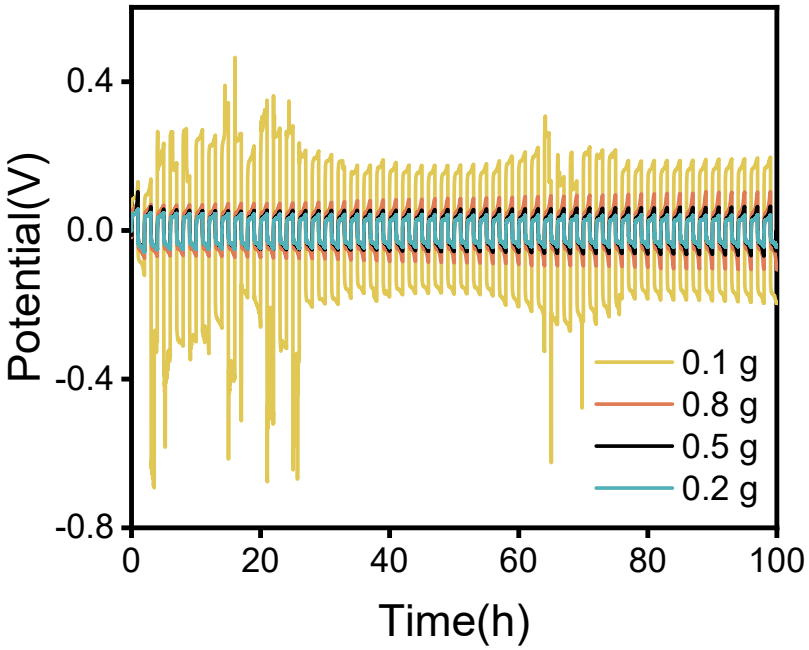

Figure S10. Long cycle curves of symmetric AlSn@Cu-0.1 g, AlSn@Cu-0.2 g, AlSn@Cu-0.5 g, AlSn@Cu-0.8 g cells at a current density of 0.5 mA cm^{-2}.

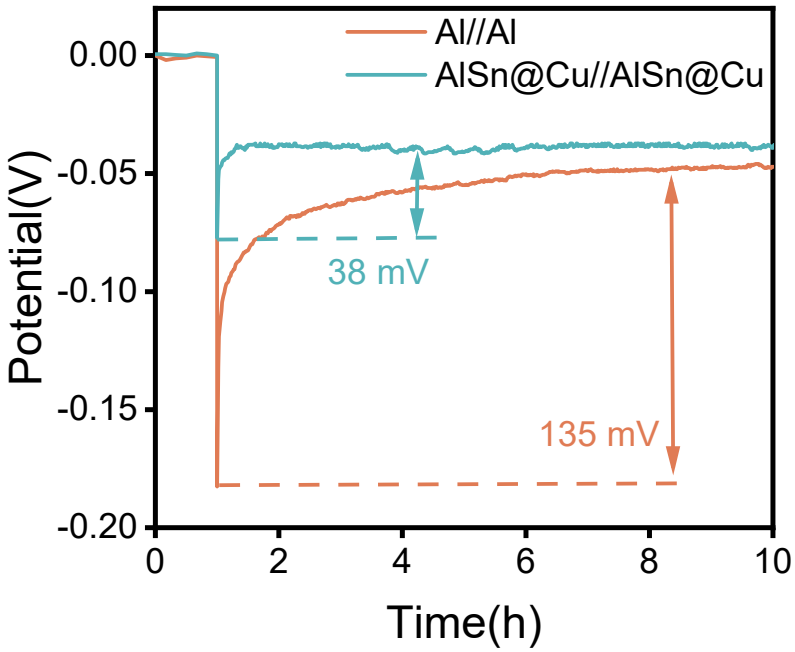

Figure S11. Voltage profiles of symmetric AlSn@Cu//AlSn@Cu and Al//Al cells at a current density of 0.2 mA cm^{-2}.

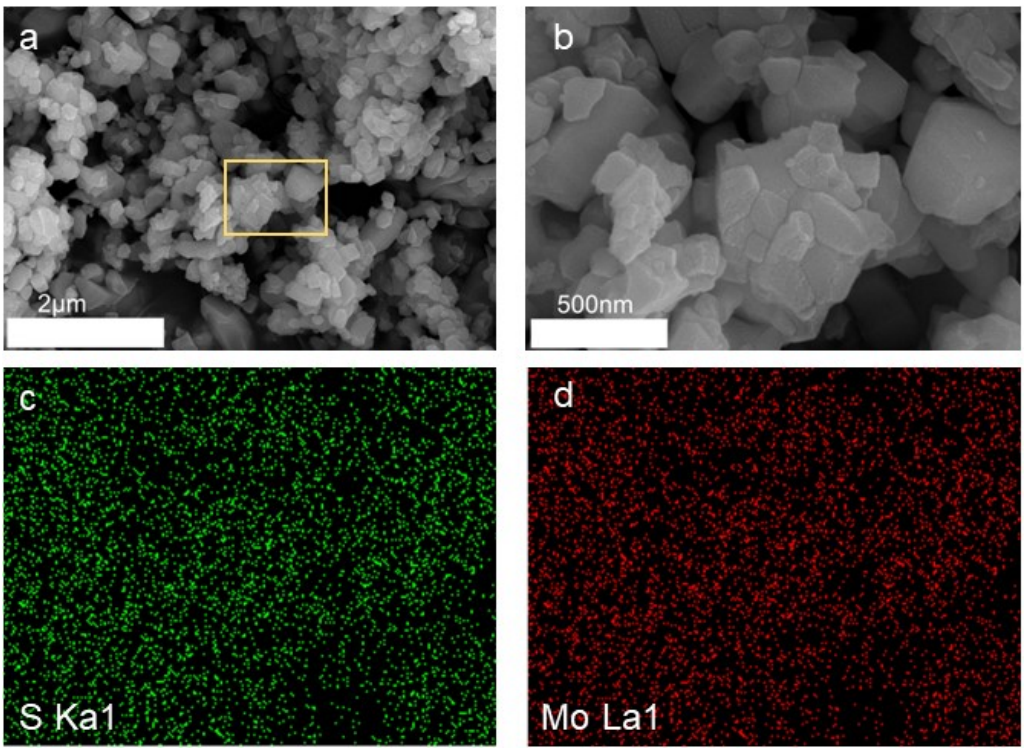

Figure S12. (a) SEM image of Mo_6S_8 cathode. (b) The enlarged SEM image in Figure S12a. EDS mappings of (c) S and (d) Mo.

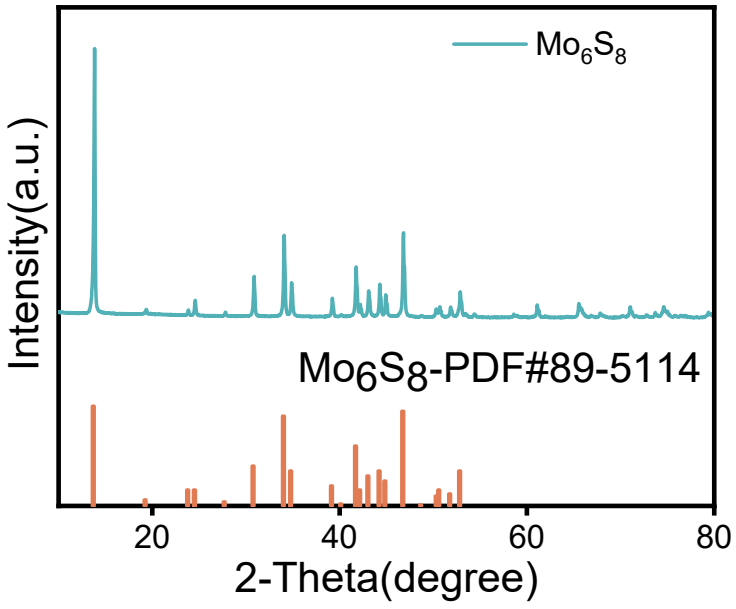

Figure S13. XRD pattern of Mo_6S_8 cathode, which can be aligned to the standard card of Mo_6S_8 (PDF#89-5114).

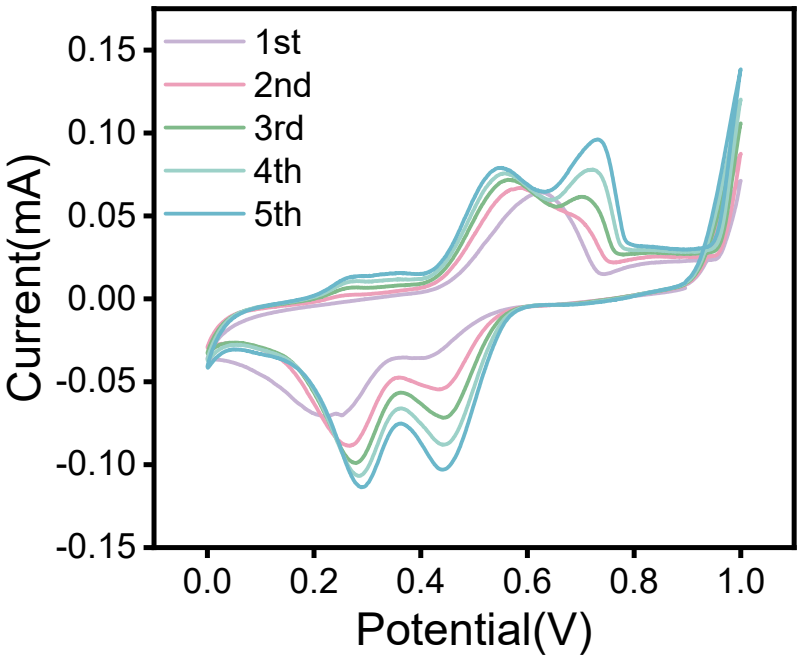

Figure S14. CV curves of AlSn@Cu// Mo_6S_8 full cell at a scan rate of 0.1 mV s^{-1}.

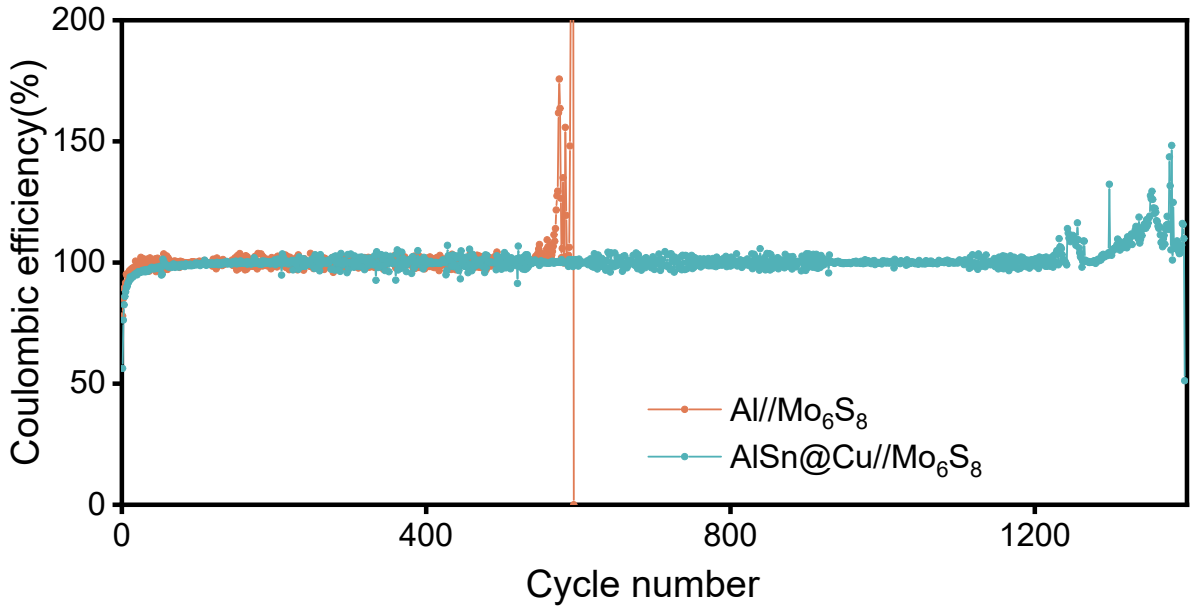

Figure S15. Coulombic efficiency of AlSn@Cu// Mo_6S_8 full cell at a current density of 100 mA g^{-1}.

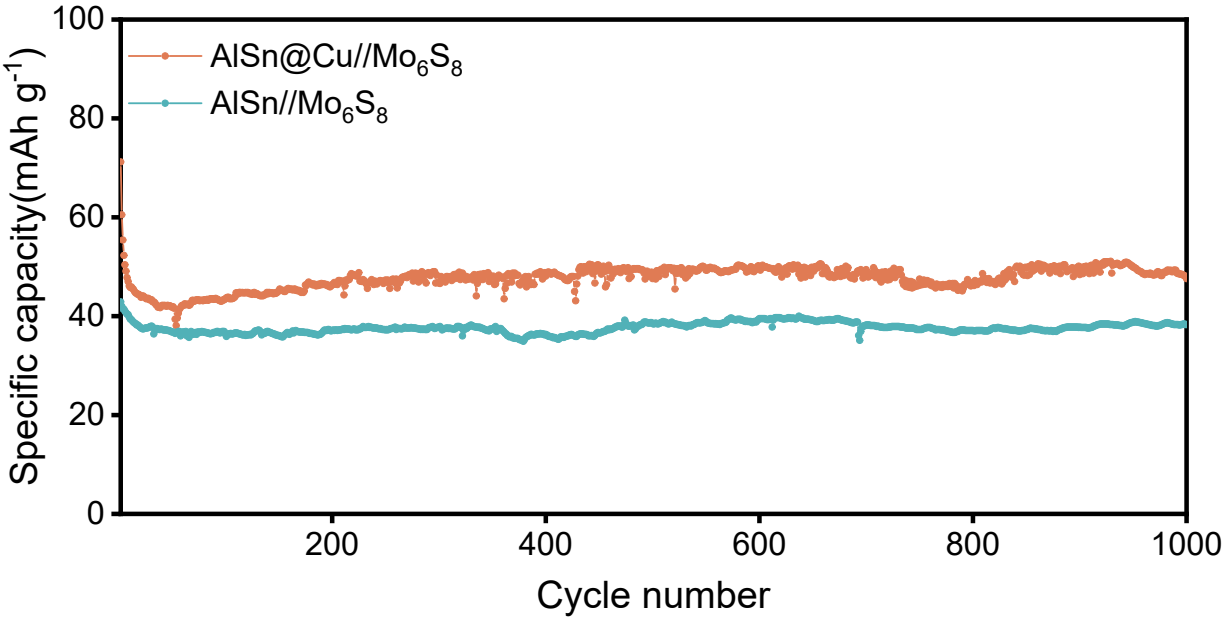

Figure S16. Long cycling curves of AlSn// Mo_6S_8 and AlSn@Cu// Mo_6S_8 full cells at 100 mA g^{-1} current density.

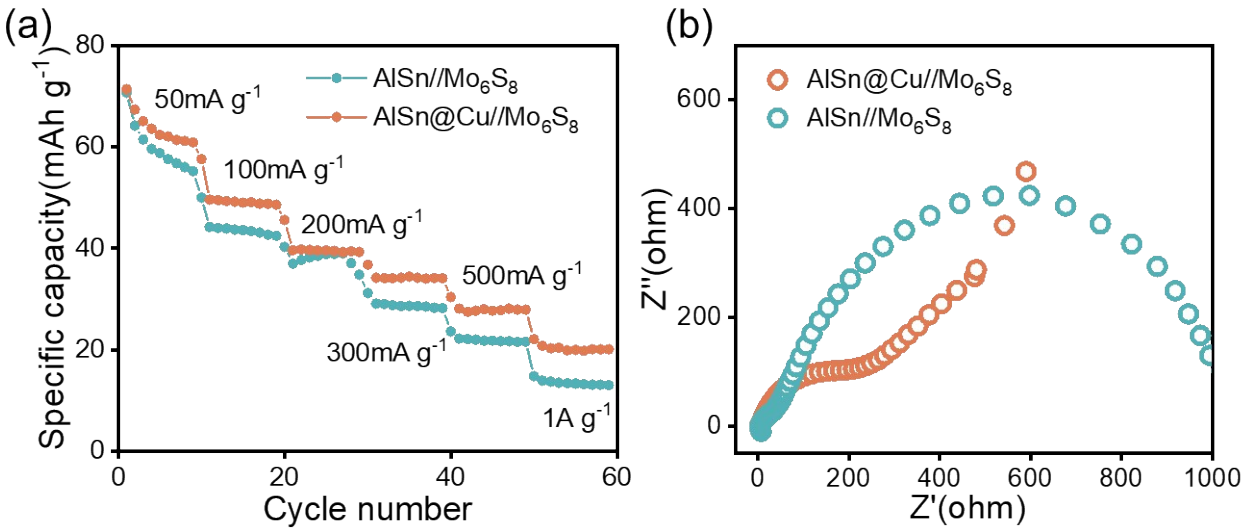

Figure S17. (a) The rate capability of AlSn// Mo_6S_8 and AlSn@Cu// Mo_6S_8 full cells at current densities of 50~1000 mA g^{-1}. (b) EIS comparison of AlSn// Mo_6S_8 and AlSn@Cu// Mo_6S_8 full cells in the range of 100 kHz~ 0.01 Hz.

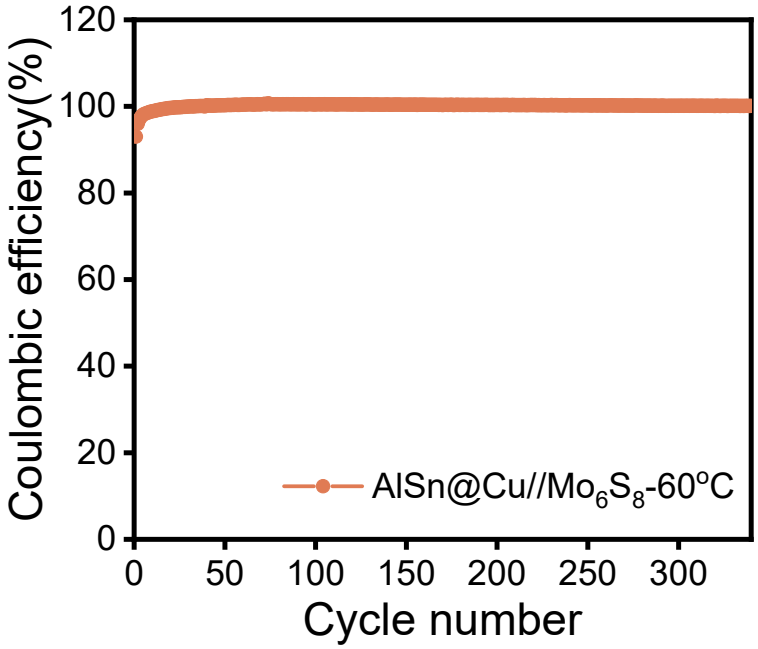

Figure S18. Coulombic efficiency of AlSn@Cu// Mo_6S_8 full cell at a current density of 100 mA g^{-1} at a high temperature of 60°C.

Table S1. EIS data fitting results of different symmetric cells.

	Cu//Cu	Al//Al	AlSn@Cu//AlSn@Cu
$R_{ct}(\Omega)$	8161	2907	896

Table S2. EIS data fitting results of AlSn@Cu symmetric cells after different cycles.

	Initial	50 cycles	100 cycles
$R_{ct}(\Omega)$	896	2.915	2.896

Table S3. The weight concentration of Al, Sn by ICP-MS with varying the addition amount of $SnCl_2$ in the molten salt electrodeposition solution.

Addition amount of $SnCl_2$ (g)	Anodes	Weight concentration (wt. %)	
		Al	Sn
0.1	AlSn@Cu-0.1 g	93.13	6.87
0.2	AlSn@Cu-0.2 g	81.25	18.75
0.5	AlSn@Cu-0.5 g	46.47	53.53
0.8	AlSn@Cu-0.8 g	33.51	66.49